frontiers | Frontiers in Marine Science

TYPE Original Research
PUBLISHED 16 September 2022
DOI 10.3389/fmars.2022.980176

OPEN ACCESS

EDITED BY
Marc Tedetti,
UMR7294 Institut Méditerranéen d'océanographie (MIO), France

REVIEWED BY
Ding He,
Zhejiang University, China
Kaijun Lu,
The University of Texas at Austin, United States

*CORRESPONDENCE
Ying Wu
wuying@sklec.ecnu.edu.cn

SPECIALTY SECTION
This article was submitted to Marine Biogeochemistry, a section of the journal Frontiers in Marine Science

RECEIVED 28 June 2022
ACCEPTED 29 August 2022
PUBLISHED 16 September 2022

CITATION
Wu Y, Koch BP, Wang X, Witt M, Wang X, Bao H, Gan S, Kattner G and Zhang J (2022) Molecular Composition of Dissolved Organic Matter in the Changjiang (Yangtze River) – Imprints of Anthropogenic Impact.
Front. Mar. Sci. 9:980176.
doi: 10.3389/fmars.2022.980176

Molecular Composition of Dissolved Organic Matter in the Changjiang (Yangtze River) – Imprints of Anthropogenic Impact

Ying Wu[1]*, Boris P. Koch[2,3], Xiaona Wang[1], Matthias Witt[4], Xiaolu Wang[1], Hongyan Bao[1,5], Shuchai Gan[1,6], Gerhard Kattner[2] and Jing Zhang[1]

[1]State Key Laboratory of Estuarine and Coastal Research, East China Normal University, Shanghai, China, [2]Alfred-Wegener-Institut Helmholtz Zentrum für Polar- und Meeresforschung, Ecological Chemistry, Bremerhaven, Germany, [3]University of Applied Science, Bremerhaven, Germany, [4]Bruker Daltonics GmbH & Co. KG, Bremen, Germany, [5]State Key Laboratory of Marine Environmental Science, Xiamen University, Xiamen, China, [6]Guangdong Provincial Key laboratory of Emergency Test for Dangerous Chemicals, Guangdong Institute of Analysis, Guangzhou, China

Understanding the biogeochemical transformation of dissolved organic matter (DOM) across fluvial networks will ultimately help to predict anthropogenic influences. To date, few studies have evaluated the anthropogenic impact on the spatial and temporal changes of DOM composition in large river systems. Here, FT-ICR-MS combined with excitation-emission matrix spectroscopy (EEMs) and biomarkers were applied to resolve chemical differences of DOM collected from the Changjiang basin at different hydrological and environmental conditions. PCA and cluster analysis illustrated that samples collected from lake systems and northern and southern tributaries differed from the two batches of main stream samples, particularly due to higher contribution of nitrogen and sulfur containing compounds. Correlation of land-use information along the tributaries with different PCA loadings indicated that agricultural, forest and wetland areas and wastewater discharge control the composition of DOM within these subregions. Higher heteroatom content (especially CHONx) in the low discharge period (2009) may be contributed by paddy soil leaching into groundwater. The relative peak magnitude of sulfur containing formulas was elevated during flood season (2010), which may be related to pollutions in areas of high population density. In addition, lignin phenol concentrations were higher in the flood season because of elevated soil erosion. Consequently, land use and human activities can strongly alter the quality and composition of DOM in watersheds flowing through densely populated regions, which may also impact or influence the riverine carbon flux in anthropogenically disturbed river systems.

KEYWORDS

DOM, molecular composition, FT-ICR-MS, Changjiang, anthropogenic

Introduction

The transport of dissolved organic matter (DOM) from rivers to the ocean represents a fundamental component of the global carbon cycle (Cole et al., 2007; Battin et al., 2009; Borisover et al., 2009; Bianchi, 2011). About 0.25 Pg of riverine dissolved organic carbon (DOC) is annually delivered from the continents to the ocean, which would be sufficient to sustain the turnover of the entire marine DOC pool (Cole et al., 2007; Aufdenkampe et al., 2011). However, dynamics of DOM within the fluvial system and its impact on the global organic carbon inventory are still insufficiently constrained (Harrison et al., 2005; Lauerwald et al., 2012; Wagner et al., 2015; Casas-Ruiz et al., 2020). Especially, a significant loss of aquatic habitats has occurred in most watersheds because of agricultural activities, urbanization, and dam constructions (Bao et al., 2015; Wagner et al., 2015; Riedel et al., 2016; Li et al., 2018a). Understanding the biogeochemical transformation of DOM across the fluvial networks will ultimately help predicting how anthropogenic influences may be altering DOM composition and turnover (Battin et al., 2008; Bao et al., 2015; Riedel et al., 2016; He et al., 2020; Zhou et al., 2021).

Riverine DOM is a heterogeneous pool of molecules from terrestrial inputs (soils and plant litters), *in-situ* production and human activities (Aufdenkampe et al., 2011; Williams et al., 2016). Significant efforts have been made towards a better understanding of biogeochemistry and seasonal dynamics of DOM in various rivers (Bianchi et al., 2004; Jaffé et al., 2012; Stubbins et al., 2015; Riedel et al., 2016; Chen et al., 2019; Lee et al., 2019). The chromophoric and fluorescent fraction of DOM (CDOM, FDOM) are subsets of DOM and ratios of optical active DOM fractions have been widely and successfully used in tracing DOM dynamics in various ecosystems (McKnight et al., 2001; Ohno, 2002; Helms et al., 2008; Stedmon and Bro, 2008; Williams et al., 2016; Richard et al., 2019). Ultrahigh-resolution Fourier transform ion cyclotron resonance mass spectrometry (FT-ICR-MS) previously provided insights into the elemental molecular composition of complex DOM supporting source and process understanding (e.g. Koch et al., 2005; Hertkon et al., 2006; Kellerman et al., 2014; Wagner et al., 2015; Riedel et al., 2016; Bahureksa et al., 2021). Chemical signatures in large rivers mirror various DOM sources and transformations, such as photo- and microbial degradation, geomorphological and hydrological processes (Roth et al., 2013; Seidel et al., 2015; Wagner et al., 2015; Riedel et al., 2016; He et al., 2020; Zhou et al., 2021). An increasing number of studies emphasizes the role of human actives on the composition of riverine DOM. This includes water quality and land use changes, as well as dam constructions, all of them as a response to increasing urbanization and intensive agriculture (Lee et al., 2019; Du et al., 2021; Shang et al., 2021; Zhou et al., 2021). However, previous reports on DOM sources and compositional properties were contradictory (e.g. with respect to contributions of microbially generated humic-like DOM or molecular compositions corresponding the influence of agricultural activities), highlighting the high spatiotemporal variability of DOM in human-influenced riverine networks (Lu et al., 2014; Singh et al., 2017; Casas-Ruiz et al., 2020). A recent study depicted the spatiotemporal patterns of the chemical diversity of DOM in a temperate system with the "Bending DOM concept", improving our knowledge of riverine DOM dynamics (Casas-Ruiz et al., 2020). However, the interrelation of complex aquatic networks within large watersheds (e.g. lakes, reservoirs and wetlands) and related modifications of DOM are still insufficiently explored (Kellerman et al., 2014; Seidel et al., 2015).

The Changjiang (Yangtze River) represents an ideal model to establish the influence of land use changes and interactions with its lake systems and groundwater on riverine DOM within the watershed. As the largest river in Asia, it has 15 major tributaries including two major lake systems (Dongting Lake and Poyang Lake) within the watershed. Croplands and industrial areas are concentrated in the mid-to-lower reaches. Numerous studies have been conducted to investigate biogeochemical characteristics of the river and human impacts on the river, e.g. the effect of the Three Gorges Dam (TGD) (Wu et al., 2007; Yu et al., 2011; Bao et al., 2015; Wu et al., 2015; Wang et al., 2019a). However, there is only limited information available on molecular-level DOM characteristics and the linkage between optical and chemical properties in dependence of environmental drivers (Wang et al., 2019b; He et al., 2020; Du et al., 2021; Zhou et al., 2021). To address the spatiotemporal dynamics of the chemical diversity of riverine DOM, it is critical to explore it in wide-basin scale coupled with different hydrological conditions, which could have comprehensive implications for the amount, composition and fate of riverine DOM.

In this study, we generated data from the Changjiang basin in two consecutive years, by combining ultrahigh-resolution mass spectrometry with optical characterization and molecular biomarkers. We aim to elucidate the impact of land-use changes and interactions among various DOM pools (lake systems and groundwater) on the composition and transformation of DOM within the large watershed. This knowledge is key for improving ecosystem and water quality management in human-affected rivers at watersheds on a global scale.

Materials and methods

Sample collection and preparation

Surface water samples (~ 0.5 m) were collected in the main stream and tributaries of the Changjiang basin in October 2009 (low discharge season, during the impoundment period of the TGD) and only in the middle- lower reaches in July–August 2010 (flood discharge season) (Figure 1). Detailed information

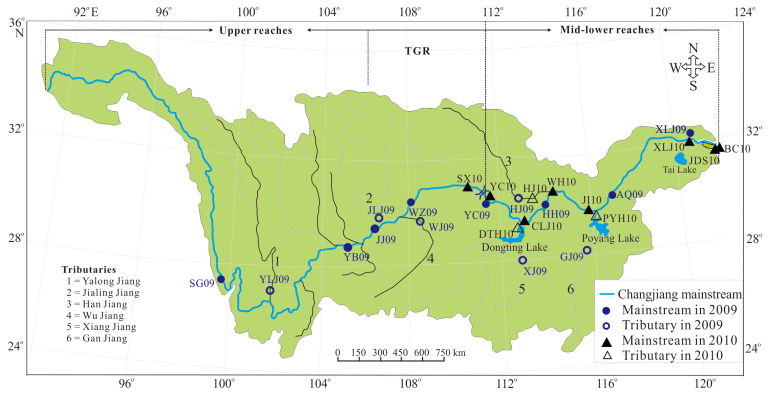

FIGURE 1
The map of sampling sites, blue dots represent the stations collected in 2009; black triangles represent the samples collected in 2010. Different numbers illustrate the tributaries in the watershed. TGR, Three Gorges Reservoir.

on the sampling can be found in Bao et al. (2015). In addition, tributaries were sampled in Wujiang (WJ), Jialingjiang (JLJ), Yalongjiang (YLJ) from the upper reaches, Hanjiang (HJ) (both years), Xiangjiang (XJ), and Ganjiang (GJ) from the middle and lower reaches. Two stations, Yichang (YC, lower reach east of the TGR and the starting point of the middle reach) and Xuliujing (XLJ, the closest station to the estuary) were selected for the detailed comparison of molecular diversity of DOM during the transport. We acquired data on surface water properties such as conductivity, nutrients, dissolved organic carbon (DOC) and nitrogen (DON), chlorophyll a (CHL), particulate organic carbon (POC), optical data (CDOM) and molecular data. The latter were bulk dissolved lignin concentration and elemental formula composition. Detailed sample handling can be referred from previous studies (Wang et al., 2019a; Zhang et al., 2020). Briefly, surface water samples were collected in the middle of the river channel and passed through pre-weighted 0.7 µm GF/F glass fiber filters (pre-combusted at 450°C for 5 h) for CHL, organic proxies and acid-cleaned polycarbonate membranes (pore size: 0.4 µm) for nutrient samples. DOC samples were filtered through 0.45 µm nylon filters (Rephile, Shanghai, China) and CDOM samples through 0.22 µm polyether sulfone filters (Millipore, Darmstadt, Germany). The filtration blanks of nylon filters and polyether sulfone filters were 3-4 µmol L^{-1} C, which is comparable with ultrapure water. Filters for CHL, POC and stable carbon isotope analysis, and samples for DOC and CDOM were kept frozen until the analysis in the lab and all samples were treated in the same way in both seasons. The filtrates for nutrients were fixed with $HgCl_2$ and stored in dark at 4°C. The filtrates (5-8 L) were collected and acidified to pH 2 to extract dissolved lignin phenols and DOM. Samples were extracted using solid phase extraction cartridges (1 g Bond Elut PPL; Agilent, CA, USA) and then eluted with 15 mL methanol according to Dittmar et al. (2008) and stored at -20°C until measurement to avoid esterification (Flerus et al., 2011). The DOC extraction efficiency ranged between 40-65%.

Chemical analyses

DOC samples were acidified and oxygen purged to remove dissolved inorganic carbon, before analysis with a total organic carbon (TOC) analyzer (Shimadzu TOC-L, Kyoto, Japan) using high-temperature catalytic oxidation (for details refer to Bao et al., 2015). The analysis of POC and stable carbon isotopes ($\delta^{13}C$ values) followed established procedures based on dried and fumed samples and analysis by an IR-MS system (Finnigan Delta-V) (Wu et al., 2015). POC% (the weight percentage of POC normalized to dry suspended particulate matter) is calculated to represent the amount of POC in the samples.

Absorption spectra for CDOM were measured with a UV–Vis spectrophotometer (Cary 100, Varian). a254 was calculated from $a_\lambda = 2.303 \times A_\lambda \div l$, where l is the path length in meters, and A_λ is the absorbance at wavelength of 254 nm, which represented the concentration of CDOM. Spectral slope coefficients, $S_{275-295}$, were calculated over the range of 275–295 nm following the exponential function and using a linear fit of a log-linearized $a_\lambda = a_{\lambda 0}\, e^{-s(\lambda-\lambda 0)}$ where λ_0 is the reference wavelength. The $S_{275-295}$ values were applied as a tracer of the DOM molecular weight, with a higher value corresponding a lower molecular weight of DOM (Helms et al., 2008). Excitation-emission matrices (EEMs) were measured with a fluorescence spectrophotometer (F-4500, Hitachi). The fluorescence index (FI; ratio of emission intensities (450 nm and 500 nm) at 370 nm excitation) yields structural features of the carbon skeleton that are influenced by the source of organic matter (McKnight et al., 2001). Parallel factor analysis (PARAFAC) was applied to decompose the spectra into individual fluorescent components

according to Stedmon and Bro (2008). Five fluorescent components were identified using the PARAFAC model with a split-half validation procedure. C1, C2, and C4 are typical humic-like components, whereas C3 and C5 are identified as protein-like components (Wang et al., 2019a). The ratio of protein-like to humic-like components (P/H) was calculated as a proxy for DOM lability. Carbon specific ultraviolet absorbance ($SUVA_{254}$, L mg C^{-1} m^{-1}) was calculated to evaluate the degree of DOM aromaticity (Ohno, 2002). All above parameters were analyzed within half year after sample collection.

Lignin phenols were determined using the CuO oxidation method as modified by Bao et al. (2015). In brief, an extracted DOM sample reacted with sodium hydroxide and an excess of CuO. After oxidation, the contents of the reaction vessels were centrifuged to separate solids from the solvent. The latter was subsequently acidified and extracted with ethyl acetate to isolate the lignin oxidation products. The concentration of lignin phenols as assessed by gas chromatography (Agilent 6890N) and the ratio of aldehyde to acid derivates of the vanilla series $(Ad/Al)_v$ was applied as a diagenetic indicator, while lig 8 represented the sum of total concentrations of vanillyl phenols (V), syringyl phenols (S), and cinnamyl phenols (C).

The concentrations total dissolved nitrogen (TDN), dissolved inorganic nitrogen (DIN; as the sum of NO_{3-}, NO_{2-}, and NH4+), DON concentration was calculated as DON = TDN-DIN. Quality control was managed with intercalibrations and repeated measurements (Liu et al., 2003; Zhang et al., 2020). CHL was extracted with acetone and measured photometrically (Bao et al., 2015).

FT-ICR-MS analysis

An FT-ICR-MS (Bruker SolariX XR, Bruker Daltonics GmbH & Co. KG, Bremen, Germany) equipped with a 12 T refrigerated actively shielded superconducting magnet and interfaced with negative ion mode electrospray ionization was used to perform ultrahigh resolution mass spectrometry analysis of DOM methanol extracts, which were diluted with water (1:1, v/v). FT-ICR-MS analyses were performed in summer 2012.

Molecular formulas were assigned using the open-access and browser-based software Ultra Mass Explorer (UME; https://ume.awi.de; Leefmann et al., 2019). Assignments were based on a pre-constructed molecular formula library (Library_02; cf. Table 1 in Leefmann et al.) and the sum of peak magnitudes having assignments explained 98.8% of the total summed peak magnitude in the sample set.

After the evaluation of the stable carbon isotope ratio precision and element specific mass accuracy, the final selection of elements were $^{1}H_{1-\infty}$, $^{12}C_{1-\infty}$, $^{14}N_{0-3}$, $^{16}O_{0-\infty}$, $^{32}S_{0-2}$ in a m/z range of 200–650 and a mass accuracy of ± 0.5 ppm. Formulas detected in four solvent and process blanks were removed from the dataset. The final dataset was validated by the presence of the main ^{13}C isotope signal, integer double bond equivalent (DBE) values and a DBE-O ≤10. In the final formula set, 99 formulas contained, both, nitrogen and sulfur atoms. These formulas showed significantly higher mass accuracy values and were not considered further in the manuscript but not removed from the dataset.

Relative peak intensities (RI) were calculated based on the base peak intensity in each sample. Intensity-weighted average parameters for each spectrum were calculated from the peak magnitude and the elemental parameters (e.g. $(O/C)_{wa}$ ratio; cf. Table 1) of each molecular formula (Koch et al., 2005). The percentage of groups of formulas, such as CHO, CHONx (x≥1), was calculated based on the percentage ratio of the number of formulas in each group versus the total number of formulas in each sample. In the supplements, we provide the full mass peak list (as.csv) and the report file (as txt file generated by UltraMassExplorer), allowing for full reproducibility of the results.

Statistical analyses

A cluster analysis was carried out using bulk and molecular parameters (e.g. DOC, stable carbon isotope ratios, lig 8, $(Ad/Al)_v$, S/V, number of molecular formulas (n(mf)), C_{wa}, S_{wa}, $(O/C)_{wa}$, $(S/C)_{wa}$, CHOSx, CHONx) and was based on the Bray–Curtis dissimilarity. A principle component analysis (PCA) was also based on major bulk parameters (DOC, lig 8, $(Ad/Al)_v$, S/V) and molecular parameters (C_{wa}, S_{wa}, $(O/C)_{wa}$, $(S/C)_{wa}$, CHOSx, CHONx etc.) and conducted to identify the elemental formulas which contributed most to the variability in the FT-ICR-MS data.

Biogeochemical parameters, optical characteristics and lignin phenol associated molecular patterns were evaluated using Spearman's rank correlation coefficients ($p< 0.05$ or $p< 0.001$). Correlation was performed between various biogeochemical parameters and relative peak intensities for each signed formula (Table S1). Parameters covered DOC, DON, optical characterization (C_1, C_2, C_3, C_4/C_2, $SUVA_{254}$ etc.) and lignin phenol parameters (lig 8, $(Ad/Al)_v$).

Path analysis of the elemental composition of DOM

Path analysis is used to evaluate causal models by examining the relationships between a dependent variable and two or more independent variables. It differentiates between correlation and causation by partitioning simple correlation coefficients between independent and dependent variables into direct and indirect effects (Du et al., 2021). Path analysis provides a numerical value for both direct and indirect effects, thus indicating the relative strength of causal relationships. Here, we conduct path analyses using the likelihood estimation method with IBM SPSS AMOS. A comparative fit index (CFI) value of > 0.9 and a root mean square error of approximation (RMSEA) of< 0.1 indicated that the path model fitted well with the data. In our models, there are

TABLE 1 Elemental parameters of dissolved organic matter collected from the Changjiang, intensity weighted average values for the formula compositions and number percentage of various groups (CHO, CHONx and CHOSx) are displayed for the comparison, X defines as ≥1.

Sample	Collected year, zone	Station	n (mf)	(mz) wa	(DBE) wa	Cwa	Hwa	Nwa	Owa	Swa	(O/C) wa	(H/C) wa	(N/C) wa	(S/C) wa	% CHO	CHONx	CHOSx
JIM10	2010, main stream	Jiujiang	2093	500	10.7	23.6	28	0.1	11.5	0.074	0.493	1.184	0.0046	0.0041	63.1	12.0	24.7
YCM10	2010, main stream	Yichang	1961	504	11	23.8	27.7	0.1	11.8	0.06	0.496	1.164	0.0045	0.0025	67.1	13.5	19.4
CLJM10	2010, main stream	Yueyang	2005	503	10.8	23.8	28.1	0.11	11.6	0.07	0.494	1.183	0.0048	0.0032	64.1	13.6	22.0
JDSM10	2010, main stream	Jiuduansha	1749	495	10.1	23.4	28.8	0.13	11.4	0.08	0.489	1.227	0.0056	0.0034	62.9	15.6	21.4
XLJM10	2010, main stream	Xulliujing	1907	483	10.2	22.9	27.6	0.1	11.1	0.08	0.487	1.202	0.0044	0.0037	66.8	11.2	21.9
WHM10	2010, main stream	Hankou	1954	494	10.5	23.4	27.9	0.09	11.4	0.07	0.491	1.189	0.0038	0.0032	68.2	10.5	21.3
SXM10	2010, main stream	Sanxia	1932	506	10.9	24	28.2	0.11	11.7	0.06	0.493	1.175	0.0045	0.0027	66.5	13.3	20.2
BCM10	2010, main stream	Beicao	1947	506	10.8	23.9	28.3	0.13	11.7	0.08	0.493	1.185	0.0055	0.0036	61.8	14.8	23.3
HJT10	2010, tributary	Hanjiang	2020	501	10.7	23.7	28.3	0.11	11.6	0.06	0.494	1.191	0.0049	0.0025	64.8	15.5	19.7
DTHT10	2010, tributary	Dongting Lake	2174	499	10.6	23.6	28.2	0.15	11.5	0.09	0.491	1.193	0.0064	0.0041	60.0	15.5	24.1
PYHT10	2010, tributary	Poyang Lake	2100	498	10.5	23.8	28.6	0.14	11.3	0.08	0.48	1.204	0.0063	0.0037	61.4	14.9	23.6
SGM09	2009, main stream	Shigu	1804	501	10.7	23.6	28	0.118	11.7	0.044	0.5	1.187	0.0051	0.0013	66.6	19.1	14.2
WZM09	2009, main stream	Wanzhou	1876	502	10.8	23.9	28.2	0.12	11.6	0.05	0.489	1.184	0.0049	0.0022	65.2	15.8	18.8
YCM09	2009, main stream	Yichang	1809	502	10.8	24.1	28.6	0.1	11.4	0.04	0.478	1.189	0.0044	0.0016	68.8	14.8	16.3
HHM09	2009, main stream	Xiantao	1758	500	10.7	23.9	28.7	0.13	11.4	0.04	0.479	1.196	0.0055	0.0017	65.7	17.3	17.0
XLJM09	2009, main stream	Xuliujing	1956	497	10.4	23.8	28.8	0.12	11.2	0.06	0.477	1.211	0.0051	0.0027	65.2	14.2	20.4
YBM09	2009, main stream	Yibin	1869	499	10.7	23.6	28	0.1	11.6	0.04	0.493	1.183	0.0046	0.0018	67.1	16.2	16.6
JJM09	2009, main stream	Jiangjin	1895	500	10.7	23.8	28.2	0.11	11.5	0.04	0.489	1.186	0.0048	0.0017	66.9	16.4	16.6
AQM09	2009, main stream	Anqing	1965	498	10.6	23.8	28.5	0.14	11.3	0.05	0.479	1.198	0.0061	0.0023	62.5	17.6	19.5
GJT09	2009, tributary	Ganjiang	1970	504	10.6	23.9	28.8	0.18	11.5	0.08	0.485	1.2	0.0077	0.0037	59.3	16.8	23.7
XJT09	2009, tributary	Xiangjiang	1897	499	10.2	24	29.9	0.18	11	0.08	0.464	1.241	0.0078	0.0034	60.6	16.3	22.6
WJT09	2009, tributary	Wujiang	1896	505	10.6	24.2	29.4	0.14	11.4	0.06	0.475	1.215	0.0059	0.0028	63.7	15.6	20.5
JLJT09	2009, tributary	Jialingjiang	1300	491	10.5	23.4	27.9	0.08	11.3	0.04	0.487	1.192	0.0036	0.0018	73.5	11.2	15.3
YLJT09	2009, tributary	Yalongjiang	1832	501	10.9	23.8	27.9	0.05	11.7	0.02	0.494	1.169	0.0022	0.001	76.4	10.9	12.7
HJT09	2009, tributary	Hanjiang	1665	501	10.5	24	29	0.1	11.4	0.03	0.478	1.208	0.0042	0.0015	68.7	15.9	15.3

The meaning of SGM09: station of Shigu (SG), as mainstream (M) station in 2009(09); HJT09: Hanjiang (HJ), as tributary (T) station in 2009(09).

not latent variables, but endogenous and exogenous variables. In the CHONx compound model, CHONx and industrial waste water are the endogenous variables. Information on agricultural population density, industrial sewage, POC and P/H are the exogenous variables. For the CHOSx compound model, population density, petroleum effluent, POC and protein-like components were involved are exogenous variables, petroleum effluent and CHOSx are the endogenous variables (Table S3).

Results and discussion

Spatiotemporal variation of the DOM composition

Terrestrial DOM is derived from multiple and heterogeneous sources such as autochthonous production and allochthonous inputs (e.g., leachates from plants and soils and organic matter

derived from human activities, respectively) and degradation (Koch et al., 2005; Martin and Harrison, 2011; Wang et al., 2012; Bao et al., 2015; Medeiros et al., 2015; Riedel et al., 2016; Zhou et al., 2021). In our study, we observed a higher average DOC concentration (139 ± 23 μmol L^{-1} DOC) in the main stream in the high discharge season of 2010 compared with the data collected in 2009 at low discharge (94 ± 20 μmol L^{-1} DOC), which were close to the previous studies collected in the similar periods (80-200 μmol L^{-1} DOC) (Bao et al., 2015; Wang et al., 2019a; Zhou et al., 2021). We also observed higher total suspended matter (TSM) concentration in 2010 than in 2009 (average values of 195 ± 90 and 160 ± 174 mg L^{-1}, respectively) and higher lig 8 (average values of 12.8 ± 4.5 and 8.7 ± 1.9 μg L^{-1}, respectively) (cf. Table S2). Doubled DON (average values of 9.5 ± 3.5 and 4.1 ± 2.1 μmol L^{-1} for 2009 and 2010, respectively) and slightly enriched $\delta^{13}C$ values were detected in samples from 2009 compared to 2010. Especially high DON concentrations (> 10 μmol L^{-1}) were observed at the middle and downstream stations in 2009. Highest values of POC% and depleted $\delta^{13}C$ values were found for most tributaries, such as GJ and XJ, and the lake systems in both seasons. Although the variability of CDOM parameters (e.g. $SUVA_{254}$) was small among the various samples, the differences of a254, C2, C4 and C5 between seasons were significant ($p< 0.05$, Table S1). In addition, the main stream samples of 2009 at the upstream and downstream stations were significantly different with respect to C1, C2, C4, and C5 ($p< 0.05$, Table S1). For samples collected from the main stream and tributaries in the two seasons, more parameters (S/V, C/V, $(Ad/Al)_v$, $\delta^{13}C$, DON) were significantly different in 2009 compared to 2010 (only TSM and S/V) ($p< 0.05$, Table S1).

Mass spectrometry yielded a total of 3,167 elemental formulas (excluding isotopologues; see Table 1) with an average of 1,893 ± 168 formulas per sample. Intensity-weighted average parameters were calculated to compare sample compositions (Table 1). In total, 334 and 289 unique formulas were determined in DOM in 2009 and 2010 (e.g. the unique formulas in 2009 means formulas not present in any sample of 2010 but present in more than one sample of 2009, respectively) with 906 formulas shared in both seasons. Among these shared formulas (observed in all samples), 87% were CHO formulas. However, among those unique formulas in 2009, 59.3% and 22.1% were CHONx and CHOSx formulas, respectively, while in 2010, the values were 36.7% and 46.7% for CHONx and CHOSx formulas. It has been previously reported that riverine DOM has a higher molecular weight and a higher state of oxygenation at elevated discharge (Raeke et al., 2017). In our dataset, we did not observe significant differences of $(O/C)_{wa}$ ratios between 2009 and 2010 for the main stream samples ($p > 0.05$). However, elevated values of $(O/C)_{wa}$ ratios were observed for the middle reach tributaries for both seasons. At low discharge in 2009, samples at station SGM09 (Shigu, most upper reach) had the highest $(O/C)_{wa}$ value among all samples. Higher N contents were found for the main stream samples in 2009 and the tributary samples of both years, with average values of 0.12 ± 0.014 (main stream, 2009), 0.12 ± 0.054 (tributaries, 2009) and 0.13 ± 0.021 (tributaries, 2010). Higher $(S/C)_{wa}$ values were mainly detected in the 2010 main stream samples, with an average of 0.0033 ± 0.0005 while it was only 0.0019 ± 0.0005 in 2009. The statistical results also indicated a high significant difference of numbers of CHONx and CHOSx formulas between the two years ($p< 0.001$). As observed in other studies (Wang et al., 2019b; He et al., 2020; Pang et al., 2021) molecular formulas consisted primarily of the CHO elemental series (59-76%), followed by sulfur (12-24%) and nitrogen containing formulas (10-19%) in most samples (Table 1). For the 2010 samples, we adjusted extraction volumes to DOC concentrations to avoid loading-dependent fractionation as Kong et al. (2021) suggested (Figure S1). The variation of $(O/C)_{wa}$ and $(H/C)_{wa}$ varied with the DOC loadings but did not differ between the two sampling periods. The similarity between the main stream and tributary stations in 2009 seems to fit with the river continuum concept (RCC) since that the diversity of DOM compounds decreased with stream order (Vannote et al., 1980). Since most tributaries and the main stream of the Changjiang are high stream order systems and anthropogenic disturbed (land use changes and dam construction), it is challenging to evaluate the RCC control on DOM diversity. Differences in the number of CHONx elemental formulas were observed between the main stream and tributary stations in 2010, and especially $(O/C)_{wa}$ and $(H/C)_{wa}$ ratios of the upper stream and middle-lower stream stations in 2009 were different (Table 1), just because that DOM compositions have also been strongly linked to watershed land cover, especially to fluvial networks (e.g. lakes and wetlands) (Roebuck et al., 2020).

Stations YC and XLJ were chosen for a direct comparison in van Krevelen diagrams to check the urbanization impact in the middle and lower reaches (Figure 2). It should be noted that even if the formulas are identical the structural diversity can be different (e.g. Pang et al., 2021). Moreover, DOM composition may have been changed during the long distance transport. Nevertheless, we found 160 and 336 unique compounds at station YC in 2009 and 2010 compared to station XLJ having 307 and 281 unique compounds in the same period. Seasonal differences of the DOM signature in the system were most pronounced at the main stream stations ($p< 0.001$, Table 1), especially with respect to the heteroatom classes and their summed relative intensity (e.g. CHONx, CHOSx etc.) as illustrated by stations YC and XLJ as an example (Figure 2). YC and XLJ belong to middle-lower streams stations, where the urbanization is elevated from the YC to XLJ, and we detected more CHO and CHOSx formulas in YC station and more CHO formulas in XLJ in 2010 during flood season. Some of these formulas contained aromatic substructures as revealed by an aromaticity index value of $AI \leq 0.5$ (Koch and Dittmar, 2006; 2016). Pang et al. (2021) observed similar phenomena and suggested that high discharge will additionally introduce a

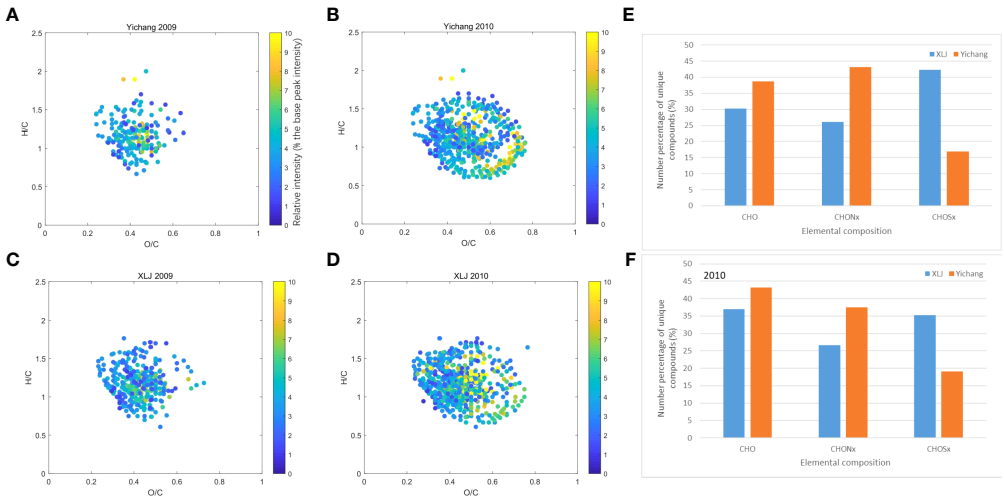

FIGURE 2
(A–D), van Krevelen diagrams of unique formulas from two stations Yichang (YC) and Xuliujing (XLJ). The color bar represents the relative intensity of each formula; **(E, F)** Comparison of number percentage of unique compounds for each of the two stations.

relatively recalcitrant pool of DOM into the Yangtze. In both seasons, these unique compounds were dominated by CHOSx and CHO series at XLJ but CHO and CHONx formulas dominated at YC (Figure 2). The number percentage of CHOSx formulas increased from YC to XLJ in both years with highly enriched characteristics in 2009 while CHO and CHONx formulas decreased from YC to XLJ. This implies that the increase in CHOSx formulas may be related to the urbanization. In a previous study, the authors observed an increased relative abundance in aliphatic molecular formulas with increasing urbanization (Zhou et al., 2021).

The variability of the DOM composition is usually highest in small headwater streams (Vannote et al., 1980; Raeke et al., 2017) caused by local sources, while the DOM composition downstream is more representative of the whole watershed processes. Three groups were roughly separated using cluster analysis (Figure 3A) and PCA (Figure 3B) based on the bulk and molecular parameters: main stream stations of 2009 and tributaries of 2009 and 2010. The samples collected from the lake systems, northern and southern tributaries were well separated from the two clusters of main stream samples, with high factor loadings, e.g. for CHONx and CHOSx compounds. Both tributary samples of the two years showed more nitrogen-containing formulas, especially in 2010, sulfur-containing formulas were more enriched in middle and lower tributaries in the two years (Table 1).

The combination of multiple parameters (e.g. CDOM, FT-ICR-MS) has been previously applied to trace the origin and transformation of DOM in the aquatic environment (Stubbins et al., 2010, 2015; Hertkorn et al., 2016; Casas-Ruiz et al., 2020; He et al., 2020). Based on previous studies, the chemical composition at the molecular level is closely associated with many spectral indicators, e.g. a_{254}, FI, $SUVA_{254}$ and florescence excitations emission matrix parallel factor components (McKnight et al., 2001; He et al., 2020). Recently it has been reported that one should be careful with such comparison analyses that were performed on original water and extracted samples (e.g., Wünsch et al., 2018; Kong et al., 2021). One detailed investigation elucidated that FT-ICR-MS formulas assigned to PARAFAC components represented ~40% of the total number of formulas identified and ~60% of total FT-ICR-MS peak intensities (Stubbins et al., 2014). Other studies, however, suggested the selective enrichment of freshwater DOM by PPL is less critical for FT-ICR-MS analysis since poorly extracted compounds also have a low response in electrospray ionization (Raeke et al., 2016). It should be noted that comparing analyses that are based on solid-phase extracts with original water analyses puts some constraints on our interpretations.

When correlating parameters in different matrices, the results can be ambiguous due to the large overlap in van Krevelen diagrams (Rivas-Ubach et al., 2018). To make our results more robust, we explored Spearman correlations of lignin phenol concentrations (Λ8, normalized by DOC concentration) with the relative magnitude of individual CHO formulas only. Significant correlations observed simultaneously in over 80% of the samples are represented in Figures 4A–D. 29.2% of CHO formulas (average molecular weight (AMW) of 540 Da) showed a high positive correlation ($r > 0.5$) withΛ8 in 2010. For the samples collected in 2009, 11.4% of formulas (AMW of 460 Da) had a negative correlation ($r< -0.5$) with Λ8 (Figures 4A, B). The correlation of the $(Ad/Al)_v$ ratio with 12.7% of CHO formulas

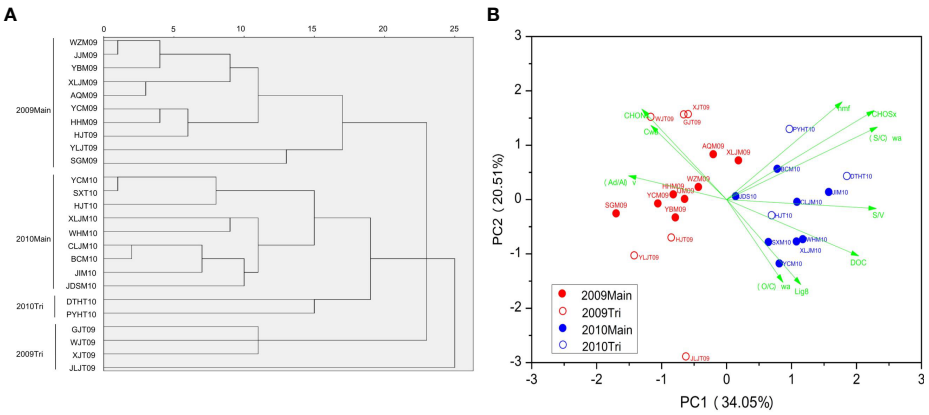

FIGURE 3
(A) Cluster analysis based on bulk and elemental signatures; **(B)** PCA analysis based on elemental information and bulk organic proxies. Tri: tributaries, Main: main stream.

(AMW of 567 Da) in 2010 also showed a positive correlation (r > 0.5), while 8.8% of CHO formulas (AMW of 395 Da) in 2009 were negatively correlated (r< -0.7) (Figures 4C, D). We noticed that those two groups differed in their distributions in VK diagrams, but were comparable with temporal variation of lig 8 and $(Ad/Al)_v$. It was reported that highly unsaturated compounds detected by FT-ICR-MS were related to soil-derived products of lignin degradation (He et al., 2020). Considering the concentrations of lignin phenols and the correlation of $(Ad/Al)_v$ with CHO%, we inferred that during high discharge (2010), terrestrial material (higher molecular weight and positive correlation with lignin phenols parameters) flushed into the river being partially degraded (Pang et al., 2021), while during low discharge (2009), autochthonous OM was more dominant as suggested by the negative correlation of lignin parameters and highly unsaturated compounds and lower AMW value (He et al., 2020). The constraints on the application of relative intensity of each formula with bulk parameters for the correlations imply that the signal abundances in the FT-ICR MS measurements affected by the experimental parameters of the instrument should be considered to ensure statistical confidence and accurately correlate the features between DOM and environment (Hawkes et al., 2020).

Mobilization and molecular transformation of DOM along the main stream

Compared to the low discharge season in 2009, we observed higher DOC, TSM and lig 8 concentrations in the main stream flood season in 2010. This can be related to elevated water discharge that results in high soil erosion as observed by Bao et al. (2015) and Pang et al. (2021). However, as reported by Raeke et al. (2017), more oxygenated and unsaturated molecular formulas are released at the high flow condition in mountainous rivers, which was not observed in our study. DBE and $(O/C)_{wa}$ values of the main stream samples were also comparable in the two seasons (Table 1). Focusing on middle and lower reach samples only, the $(O/C)_{wa}$ values were significantly higher in 2010 than 2009, which may be related to the variation of DOM sources between the two years. Figure 5 demonstrated the relationship of bulk chemical parameters (DOC, TSM and DOC/DON ratio) and elemental information ($(H/C)_{wa}$, $(O/C)_{wa}$). The correlation of $(H/C)_{wa}$ and $(O/C)_{wa}$ with DOC was significantly different between 2009 and 2010 (r = 0.62 and r = 0.70 for $(H/C)_{wa}$ *vs* DOC; r = 0.90 and r = 0.60 for $(O/C)_{wa}$ *vs* DOC). In 2009, DOC showed a weak positive correlation with $(H/C)_{wa}$ (p< -0.1) in contrast to 2010 where it was negatively correlated (p< 0.05). In main stream samples, $(O/C)_{wa}$ showed a weak positive correlation (p = 0.05) with DOC in 2010 and a negative correlation in 2009 (p< 0.05). This implies that more hydrogenated compounds dominated in samples with higher DOC concentration in 2009, while more unsaturated compounds accumulated with higher DOC concentrations in 2010 (Figures 5A, B). This observation matches with previous observations in the Changjiang Estuary (Pang et al., 2021).

The temporal distribution patterns of molecular signatures shown by $(O/C)_{wa}$ values in 2010 were more uniform but more oxygenated in samples with lower DOC concentration in 2009 (Figure 5B). This suggests that, in contrast to small or mountainous rivers, in large river systems, such as the Changjiang, the signature of DOM may not simply be driven by discharge. The recent pulse-shunt concept (PSC) suggests that large river systems have their own characteristics due to the increase in concentration and decrease in residence time with flooding events (Casas-Ruiz et al., 2020), both the pulse and the

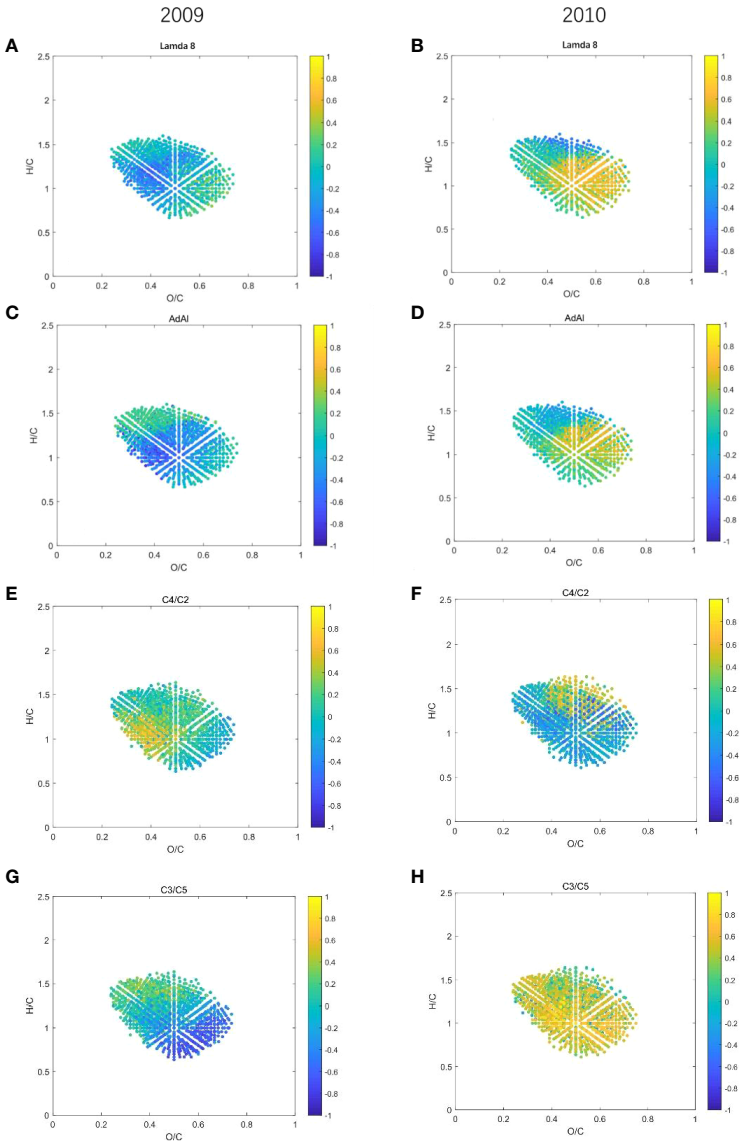

FIGURE 4
van Krevelen diagram: Colors represent the Spearman correlation coefficient for three parameters tested against relative intensity change of each molecular formula in the data set. Correlation analyses were performed for 2009 (left panels) and 2010 (right panels) samples. **(A B)**: Λ8 vs CHO formulas; **(C D)**: $(Ad/Al)_v$ vs CHO formulas; **(E, F)**: C4/C2 vs all formulas; **(G, H)**: C3/C5 vs all formulas.

shunt were accentuated by event, compounding the importance of big rivers for the removal of terrestrial DOM at annual scales (Raymond et al., 2016). Here, the signature of DOM is more likely coupled with source (in 2009) and hydrological network (in 2010). Furthermore, high DON concentrations observed in 2009 indicated the potential contribution of groundwater (about 11% of the increased discharge between Yichang and Datong) due to the impoundment of the Three Gorges Dam estimated previously from the water budget of the middle and lower reaches of the river at high DOM concentrations (Yu et al., 2018; Liang et al., 2022). It has been reported that groundwater can play an important role in the compensation of runoff reduction due to droughts or impoundment in the Yangtze River. About 31% of the increased discharge between Yichang and Datong could be contributed from the groundwater discharge as observed in 2006 (Dai et al., 2010). Cluster analysis (Figure 3A) also demonstrated the dissimilarity in elemental formula compositions of main stream and tributary samples in 2009 but similar formula compositions in 2010. The correlation of $(C/N)_{wa}$ and TSM concentrations (Figure 5C) differed between three sample subgroups: main stream samples in 2010 showed no change in $(C/N)_{wa}$ over TSM concentrations,

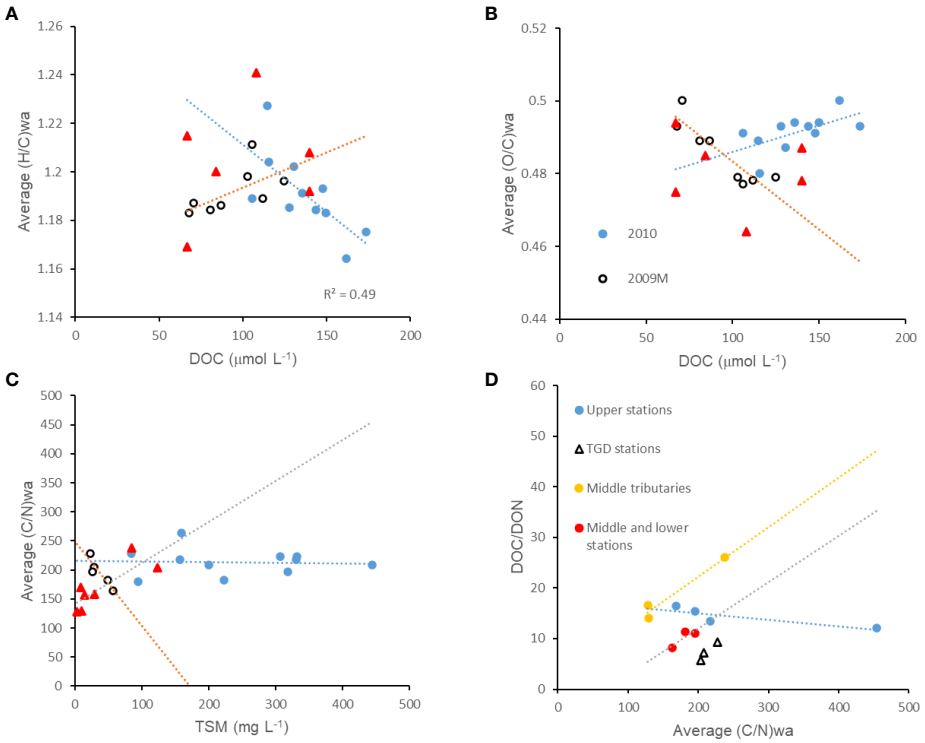

FIGURE 5
Linear correlations of bulk parameters with elemental proxies subdivided into various sample groups. **(A)**: DOC vs $(H/C)_{wa}$; **(B)**: DOC vs $(O/C)_{wa}$; **(C)**: TSM vs $(C/N)_{wa}$; **(D)**: DOC/DON vs $(C/N)_{wa}$.

while the other two groups (tributaries and 2009 main stream samples in middle and lower regions) with low TSM values were linearly correlated with $(C/N)_{wa}$ ($p< 0.05$). We speculate that this is due to dominant autochthonous processes in the tributaries and a dilution effect of terrestrial input or groundwater in the 2009 main stream samples. The correlation of the DOC/DON ratio with a $(C/N)_{wa}$ of the subgroup samples in 2009 showed contrasting trend between upper stream samples and middle/lower stations & tributaries ($p< 0.05$) (Figure 5D). The interference of upper stream samples on middle and lower reach samples was limited due to TGD operation in 2009. Combined with the characteristics of the tributaries and middle and lower reaches samples (more oxygenated compositions and lower $S_{275–295}$), such observation implies another independent source could not be denied with low DOC/DON ratios, which we infer that could be contributed by groundwater. As previous study indicated, most groundwater samples show more aromaticity and higher molecular weight in DOM composition than surface water samples (Huang et al., 2015).

Once terrestrial DOM is released into the aquatic environment, photo-degradation and microbial decomposition are important processes that modify the original DOM signature, especially in large fluvial system, where the residence time is long (Sleighter et al., 2014; Wagner et al., 2015; Seidel et al., 2015; Wang et al., 2019a). The ratio of C4/C2 was calculated to indicate photo-degradation. Previous studies suggest that higher values are representative for higher photo-degradation (Hansen et al., 2016). Again, when evaluating the Spearman correlation between the C4/C2 and C3/C5 ratios with various elemental formulas, we only chose significant correlations observed simultaneously in more than 80% of samples. We observed a positive correlation ($r > 0.5$) of C4/C2 with 12.4% of formulas of AMW of 476 Da and average DBE of 11.6 in 2009, responding to relative efficient photo-degradation due to lower TSM values in 2009. A negative correlation ($r< -0.5$) of C4/C2 with 7% of formulas with AMW of 553 Da and average DBE of 11.2, which resisted photo-degradation, was observed in 2010, only a small portion of formulas with $(H/C)_{wa} > 1.5$ showed a positive correlation with C4/C2 (Figures 4E, F). C3 and C5 fractions were considered as tyrosine-like and tryptophan-like components with higher bioavailability (Yamashita et al., 2011; Painter et al., 2018). The ratio of C3/C5 has been applied to evaluate the diagenetic state of DOM due to microbial degradation, as lower values indicate higher decomposition. The average values of C3/C5 in 2009 and 2010 were 1.20 ± 0.28 and 0.76 ± 0.09, respectively. Van Krevelen

diagrams demonstrated the difference of elemental formula composition by microbial degradation between the two years (Figures 4G, H). In 2009, only 16.2% of formulas (depleted in H/C and enriched in O/C) had a significant negative correlation with the C3/C5 ratio (r< -0.5). But in 2010, 50% of all formulas with AMW of 540 Da and average DBE of 11.9 were positively correlated (r > 0.5) and among them about 14.8% contained N and S (Figures 4G, H). Visualization of VK diagram of such correlation should be carefully interpreted and better to complement the results with the information of molecular weight and DBE values, which often is lost in such a two-dimensional diagram. In summary, in 2009 the modification, transformation and degradation of DOM was dominated by photo-degradation supported by the bulk and spectral characteristics, the low flow velocity and low suspended matter content. In 2010, in contrast, the transformation in DOM was dominated by microbial degradation, additionally shown by the degradation of CDOM (C3/C5 ratios) as well as dissolved lignin components ($(Ad/Al)_v$ ratios).

Land use effect and pollution impact on DOM molecular characteristics

Agricultural activities (e.g. paddy field) dominate in the middle and lower reaches of the Changjiang. It is an ideal scenario to evaluate the potential influence of paddy soils on riverine DOM (Li et al., 2018a). In addition, rapid economic development and urbanization are unavoidable processes within the watershed. It has been previously suggested that land-use is one of the main drivers for the reactivity and molecular composition of riverine DOM (Li et al., 2018b). When we compare the signature of DOM collected from tributaries and main stream, especially by the elemental formulas, they were well separated illustrated by cluster analysis (Figure 3A). PCA analysis showed similar results, even when combined with bulk chemical properties (Figure 3B). The samples collected from lake systems, northern and southern tributaries were well separated from the two batches of main stream samples. The 2009 main stream samples had high positive PC1 scores and those from 2010 had high negative PC2 scores (Figure 3B).

Together, the four PCA loadings accounted for nearly 82% of the total variance. Correlation of land-use information of the tributaries with PCA loadings are illustrated in Figures 6A, B, D. Among them, the variations of agricultural, forest and wetland areas correlated with score 1 (38.7%), 2 (20.0%) and 4 (9.7%). Score 3 (13.1%) showed a good correlation with industrial sewage from sub-watersheds of the Changjiang (southern tributaries (Ganjiang, Xiangjiang, Wujiang) and northern tributaries (Hanjiang, Jialingjiang) etc.) (Figure 6C, the related detailed information was listed in Table S3). Riverine DOM derived from forest areas was reported to be more oxygenated, more aromatic and higher in molecular weight (Wagner et al., 2015). The molecular formula composition of our upper reach stations, such as SGM09, WZM09 and the tributaries (WJT09, YLJT09) agreed to these results, due to their strong impact by terrestrial-plant-derived material from forested areas (Table 1). Paddy soil DOM is characterized by higher N-containing compounds and lignin and aromatic components, due to soil-derived humics (Li et al., 2018a). CHONx formulas were enriched in the tributary samples (WJT09, XJT09, GJT09, HJT09) where paddy soil from the watersheds contributed to DOM.

Lacustrine-derived DOM samples are usually dominated by CHO formulas (>70%) but may have also a high heteroatom content (Goldberg et al., 2015). In our study, CHONx and CHOSx formulas occurred more often in lacustrine-derived DOM samples (DTHT10, PYHT10 and GJT09 and XJT09; Table 1), which is in agreement with higher DON concentrations. Nitrogen can become part of DOM *via* biological production of strong organic N-containing nucleophiles and/or *via* abiotic and biotic process (Sleighter et al., 2014). In our 2009 samples however, we observed elevated concentrations of DON but not of lignin phenols, which may be due to the significant contribution of DON from leaching of paddy soils to groundwater in this region (Wang et al., 2019a) being discharged to the riverine system. The path analysis model of CHONx also confirmed this assumption (Figure 7A). We found that CHONx formulas were correlated with agricultural population density, POC and P/H (as an indicator for DOM lability), which are related to the agricultural activities and *in situ* production, respectively. Agricultural population density had the largest effect on the CHONx formulas, as shown by its standardized path coefficient of 1.09. P/H also had a significant impact on the CHONx formulas as indicator of *in situ* production. The path coefficient of P/H was 0.37, which was higher than that of POC.

Effluent organic matter can yield CHOSx formulas due to the presence of surfactants such as linear alkyl benzene sulfonates (Lechtenfeld et al., 2013). In our data integration, we have removed all formulas that match the elemental composition of surfactants due to the uncertainties of their potential sources (directly derived from the environments or only enriched in surface layer etc.; Lechtenfeld et al., 2013). However, 25% of all formulas still contained sulfur, with a PC3 maximum loading being higher than that of CHONx formulas. Heteroatom-rich refinery process water could be responsible for the high PC3 loading as well as wastewater discharge to the tributaries (Li et al., 2015). Pathway analysis showed that the CHOSx formulas were also affected by petroleum effluent (Figure 7B). Petroleum effluent is rich in sulfur (Lechtenfeld et al., 2013), however, it had a negative effect on the CHOSx formulas in this study. This might be related to the fact that the petroleum effluent was a point source of CHOSx, and may be diluted by the river flow. The total effect of the population density (net path coefficient) on CHOSx formulas was 0.60,

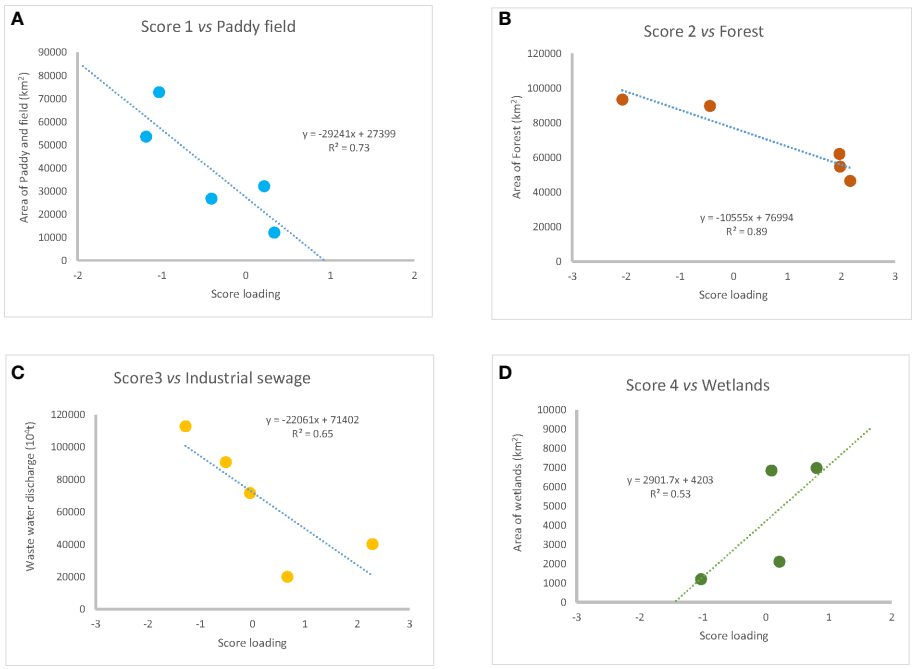

FIGURE 6
Correlation of PCA loadings of molecular structures with land use/anthropogenic input information in various tributaries, **(A)**: Paddy field; **(B)**: Forest; **(C)**: Industrial waste water;-**(D)**: Wetlands.

while the direct and indirect effects were 1.99 and -1.39 (which generate from the multiplication of two direct factors, 0.95×(-1.46)), respectively. Recent studies indicated that CHOS molecules in urban organic aerosols are highly related to anthropogenic emissions (e.g. cooking and/or biogenic primary emissions) (Su et al., 2022). The population density had a significant positive effect on the contribution of CHOSx formulas, which indicated that human activities act as a potential source of CHOSx and that CHOSx is generally better accumulated and released in high discharge periods.

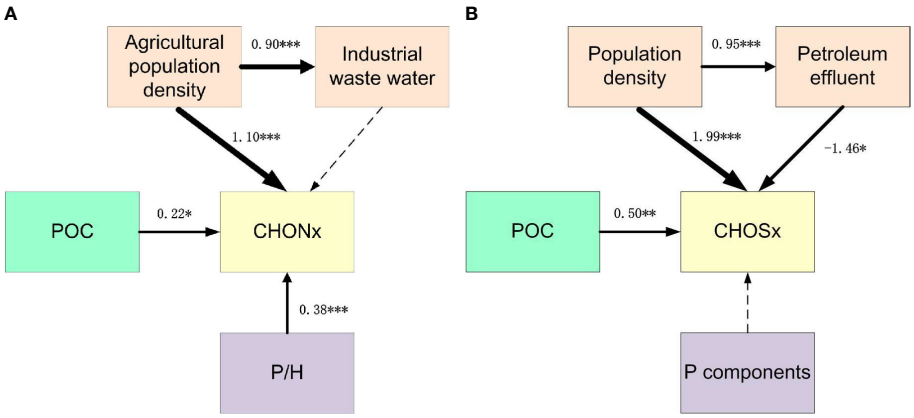

FIGURE 7
Path diagrams estimating direct and indirect effects on DOM elemental compositions. **(A)** Effects on CHONx; **(B)** Effects on CHOSx. Solid lines represent significant effects ($p<0.05$), and dashed lines represent insignificant effects. Numbers adjacent to the arrows are standardized path coefficients, *$p<0.05$, **$p<0.01$, ***$p<0.001$).

Conclusions

Hydrological and biogeochemical controls on watershed DOM transport in the Anthropocene is complex and often difficult to predict. We observed that in the Changjiang basin different landscape functional units (e.g. reservoirs, wetlands, land use pattern) had an impact on the composition of DOM. In our study, the DOM signature from the upper reach was mainly reduced by TGD, especially in the dry season. In the same period, lake, wetland and groundwater systems in the middle and lower reaches made an important contribution to the DOM pool and the occurrence of CHONx formulas. In the high discharge period, the "Passive pipe" (short residence time and extreme connectivity) showed a relatively conservative behavior with additional inputs from anthropogenic disturbances, especially for CHOSx formulas being elevated in 2010, which links to density of humans and related pollutions. These findings suggest that human activities and land use changes impact the chemical composition of DOM and play an important role C, N and S cycling in watersheds.

Data availability statement

The original contributions presented in the study are included in the article/Supplementary Material. Further inquiries can be directed to the corresponding author.

Author contributions

YW and JZ contributed to the research design. XNW, HB and SG contributed to sample collection. YW and XNW performed data analyses and interpretation. BK performed FT-ICR-MS acquisition and data analyses. MW provided support for the FTICR/MS analyses. XLW provided the plots support. YW, BK, GK and JZ wrote the manuscript. All authors provided significant input on the final manuscript.

Acknowledgments

The authors acknowledge the research funding provided by the Natural Science Foundation of China (No. 41876074, 41530960 and 41021064) and the Research Funds of Happiness Flower ECNU (20212110) and 111 project (BP0820020). YW is thankful to the support of Alexander Humboldt Fellowship. The authors are grateful to our colleagues of State Key Laboratory of Estuarine and Coastal Research (SKLEC) (East China Normal University) as well as Ecological Chemistry Group of the Alfred Wegener Institute. The authors highly appreciated the comments and suggestions given by the reviewers.

Conflict of interest

Author MW is employed by Bruker Daltonik GmbH.

The remaining authors declare that the research was conducted in the absence of any commercial or financial relationships that could be construed as a potential conflict of interest.

Publisher's note

All claims expressed in this article are solely those of the authors and do not necessarily represent those of their affiliated organizations, or those of the publisher, the editors and the reviewers. Any product that may be evaluated in this article, or claim that may be made by its manufacturer, is not guaranteed or endorsed by the publisher.

Supplementary material

The Supplementary Material for this article can be found online at: https://www.frontiersin.org/articles/10.3389/fmars.2022.980176/full#supplementary-material

References

Aufdenkampe, A. K., Mayorga, E., Raymond, P. A., Melack, J. M., Doney, S. C., Alin, S. R., et al. (2011). Riverine coupling of biogeochemical cycles between land, oceans, and atmosphere. *Front. Ecol. Environ.* 9 (1), 53–60. doi: 10.1890/100014

Bahureksa, W., Tfaily, M. M., Boiteau, R. M., Young, R. B., Logan, M. N., McKenna, A. M., et al. (2021). Soil organic matter characterization by Fourier transform ion cyclotron resonance mass spectrometry (FTICR MS): A critical review of sample preparation, analysis, and data interpretation. *Environ. Sci. Technol.* 55 (14), 9637–9656. doi: 10.1021/acs.est.1c01135

Bao, H., Wu, Y., and Zhang, J. (2015). Spatial and temporal variation of dissolved organic matter in the changjiang: Fluvial transport and flux estimation. *J. Geophys. Res. Biogeosci.* 120 (9), 1870–1886. doi: 10.1002/2015JG002948

Battin, T. J., Kaplan, L. A., Findlay, S., Hopkinson, C. S., Marti, E., Packman, A. I., et al. (2008). Biophysical controls on organic carbon fluxes in fluvial networks. *Nat. Geosci.* 1 (2), 95–100. doi: 10.1038/ngeo101

Battin, T. J., Luyssaert, S., Kaplan, L. A., Aufdenkampe, A. K., Richter, A., and Tranvik, L. J. (2009). The boundless carbon cycle. *Nat. Geosci.* 2 (9), 598–600. doi: 10.1038/ngeo618

Bianchi, T. S. (2011). The role of terrestrially derived organic carbon in the coastal ocean: A changing paradigm and the priming effect. *Proc. Natl. Acad. Sci.* 108 (49), 19473–19481. doi: 10.1073/pnas.10179821

Bianchi, T. S., Filley, T., Dria, K., and Hatcher, P. G. (2004). Temporal variability in sources of dissolved organic carbon in the lower Mississippi river. *Geochim. Cosmochim. Acta* 68 (5), 959–967. doi: 10.1016/j.gca.2003.07.011

Borisover, M., Laor, Y., Parparov, A., Bukhanovsky, N., and Lado, M. (2009). Spatial and seasonal patterns of fluorescent organic matter in lake kinneret (Sea of Galilee) and its catchment basin. *Water Res.* 43 (12), 3104–3116. doi: 10.1016/j.watres.2009.04.039

Casas-Ruiz, J. P., Spencer, R. G., Guillemette, F., von Schiller, D., Obrador, B., Podgorski, D. C., et al. (2020). Delineating the continuum of dissolved organic

matter in temperate river networks. *Global Biogeochem. Cycles* 34 (8), e2019GB006495. doi: 10.1029/2019GB006495

Chen, M., Li, C., Zeng, C., Zhang, F., Raymond, P. A., and Hur, J. (2019). Immobilization of relic anthropogenic dissolved organic matter from alpine rivers in the Himalayan-Tibetan plateau in winter. *Water Res.* 160, 97–106. doi: 10.1016/j.watres.2019.05.052

Cole, J. J., Prairie, Y. T., Caraco, N. F., McDowell, W. H., Tranvik, L. J., Striegl, R. G., et al. (2007). Plumbing the global carbon cycle: Integrating inland waters into the terrestrial carbon budget. *Ecosystems* 10 (1), 172–185. doi: 10.1007/s10021-006-9013-8

Dai, Z., Du, J., Chu, A., Li, J., Chen, J., and Zhang, X. (2010). Groundwater discharge to the changjiang river, China, during the drought season of 2006: Effects of the extreme drought and the impoundment of the three gorges dam. *Hyd. J.* 18, 359–369. doi: 10.1007/s10040-009-0538-8

Dittmar, T., Koch, B., Hertkorn, N., and Kattner, G. (2008). A simple and efficient method for the solid-phase extraction of dissolved organic matter (SPE-DOM) from seawater. *Limnol. Oceanogr. Methods* 6 (6), 230–235. doi: 10.4319/lom.2008.6.230

Du, Y., Lu, Y., Roebuck, J. A.Jr., Liu, D., Chen, F., Zeng, Q., et al. (2021). Direct versus indirect effects of human activities on dissolved organic matter in highly impacted lakes. *Sci. Total Environ.* 752, 141839. doi: 10.1016/j.scitotenv.2020.141839

Flerus, R., Koch, B. P., Schmitt-Kopplin, P., Witt, M., and Kattner, G. (2011). Molecular level investigation of reactions between dissolved organic matter and extraction solvents using FT-ICR MS. *Mar. Chem.* 124, 100–107. doi: 10.1016/j.marchem.2010.12.006

Goldberg, S., Ball, G., Allen, B., Schladow, S., Simpson, A., Masoom, H., et al. (2015). Refractory dissolved organic nitrogen accumulation in high-elevation lakes. *Nat. Comun.* 6 (1), 1–9. doi: 10.1038/ncomms7347

Hansen, A. M., Kraus, T. E., Pellerin, B. A., Fleck, J. A., Downing, B. D., and Bergamaschi, B. A. (2016). Optical properties of dissolved organic matter (DOM): Effects of biological and photolytic degradation. *Limnol. Oceanogr.* 61 (3), 1015–1032. doi: 10.1002/lno.10270

Harrison, J. A., Caraco, N., and Seitzinger, S. P. (2005). Global patterns and sources of dissolved organic matter export to the coastal zone: Results from a spatially explicit, global model. *Global Biogeochem. Cycles* 19 (4), 1–16. doi: 10.1029/2005GB002480

Hawkes, J. A., d'Andrilli, J., Agar, J. N., Barrow, M. P., Berg, S. M., Catalan, N., et al. (2020). An international laboratory comparison of dissolved organic matter composition by high resolution mass spectrometry: Are we getting the same answer? *Limnol. Oceanogr.- Meth.* 18 (6), 235–258. doi: 10.1002/lom3.10364

Helms, J. R., Stubbins, A., Ritchie, J. D., Minor, E. C., Kieber, D. J., and Mopper, K. (2008). Absorption spectral slopes and slope ratios as indicators of molecular weight, source, and photobleaching of chromophoric dissolved organic matter. *Limnol. Oceanogr.* 53 (3), 955–969. doi: 10.4319/lo.2008.53.3.0955

Hertkorn, N., Benner, R., Frommberger, M., Schmitt-Kopplin, P., Witt, M., Kaiser, K., et al. (2006). Characterization of a major refractory component of marine dissolved organic matter. *Geochim. Cosmochim. Acta* 70 (12), 2990–3010. doi: 10.1016/j.gca.2006.03.021

Hertkorn, N., Harir, M., Cawley, K., Schmitt-Kopplin, P., and Jaffé, R. (2016). Molecular characterization of dissolved organic matter from subtropical wetlands: A comparative study through the analysis of optical properties, NMR and FTICR/MS. *Biogeosci.* 13, 2257–2277. doi: 10.5194/bg-13-2257-2016

He, D., Wang, K., Pang, Y., He, C., Li, P., Li, Y., et al. (2020). Hydrological management constraints on the chemistry of dissolved organic matter in the three gorges reservoir. *Water Res.* 187, 116413. doi: 10.1016/j.watres.2020.116413

Huang, S., Wang, Y., Ma, T., Tong, L., Wang, Y., Liu, C., et al. (2015). Linking groundwater dissovled organic matter to sedimentary organic matter from a fluvio-lacustrine aquifer At jianghan plain, China by EEM-PARAFAC and hydrochemical analyses. *Sci. Total Environ.* 529, 131–139. doi: 10.1016/j.scitotenv.2015.05.051

Jaffé, R., Yamashita, Y., Maie, N., Cooper, W., Dittmar, T., Dodds, W., et al. (2012). Dissolved organic matter in headwater streams: Compositional variability across climatic regions of north America. *Geochim. Cosmochim. Acta* 94, 95–108. doi: 10.1016/j.gca.2012.06.031

Kellerman, A. M., Dittmar, T., Kothawala, D. N., and Tranvik, L. J. (2014). Chemodiversity of dissolved organic matter in lakes driven by climate and hydrology. *Nat. Comun.* 5 (1), 1–8. doi: 10.1038/ncomms4804

Koch, B. P., and Dittmar, T. (2006). From mass to structure: An aromaticity index for high-resolution mass data of natural organic matter. *Rapid Commun. Mass Spectrom.* 20 (5), 926–932. doi: 10.1002/rcm.2386

Koch, B. P., and Dittmar, T. (2016). From mass to structure: An aromaticity index for high-resolution mass data of natural organic matter. *Rapid Commun. Mass Spectrom.* 30, 250–250. doi: 10.1002/rcm.7433

Koch, B. P., Witt, M., Engbrodt, R., Dittmar, T., and Kattner, G. (2005). Molecular formulae of marine and terrigenous dissolved organic matter detected by electrospray ionization Fourier transform ion cyclotron resonance mass spectrometry. *Geochim. Cosmochim. Acta* 69 (13), 3299–3308. doi: 10.1016/j.gca.2005.02.027

Kong, X., Jendrossek, T., Ludwichowski, K., Marx, U., and Koch, B. P. (2021). Solid-phase extraction of aquatic organic matter: Loading-dependent chemical fractionation and self-assembly. *Environ. Sci. Technol.* 55 (22), 15495–15504. doi: 10.1021/acs.est.1c04535

Lauerwald, R., Hartmann, J., Ludwig, W., and Moosdorf, N. (2012). Assessing the nonconservative fluvial fluxes of dissolved organic carbon in north America. *J. Geophys. Res. Biogeosci.* 117 (G1), 1–19. doi: 10.1029/2011JG001820

Lechtenfeld, O. J., Koch, B. P., Gašparović, B., Frka, S., Witt, M., and Kattner, G. (2013). The influence of salinity on the molecular and optical properties of surface microlayers in a karstic estuary. *Mar. Chem.* 150, 25–38. doi: 10.1016/j.marchem.2013.01.006

Leefmann, T., Frickenhaus, S., and Koch, B. P. (2019). UltraMassExplorer: A browser-based application for the evaluation of high-resolution mass spectrometric data. *Rapid Commun. Mass Spectrom.* 33 (2), 193–202. doi: 10.1002/rcm.8315

Lee, M. H., Lee, Y. K., Derrien, M., Choi, K., Shin, K. H., Jang, K. S., et al. (2019). Evaluating the contributions of different organic matter sources to urban river water during a storm event *Via* optical indices and molecular composition. *Water Res.* 165, 115006. doi: 10.1016/j.watres.2019.115006

Liang, Y., Nghiem, A., Xu, J., Tang, L., Wei, W., Prommer, H., et al. (2022). Sources of ammonium enriched in groundwater in the central Yangtze river basin: Anthropogenic or geogenic? *Environ. Pollu.* 306, 119463. doi: 10.1016/j.envpol.2022.119463

Li, L., He, Z. L., Tfaily, M. M., Inglett, P., and Stoffella, P. J. (2018b). Spatial-temporal variations of dissolved organic nitrogen molecular composition in agricultural runoff water. *Water Res.* 137, 375–383. doi: 10.1016/j.watres.2018.01.035

Li, X. M., Sun, G. X., Chen, S. C., Fang, Z., Yuan, H. Y. , Shi, Q., et al. (2018a). Molecular chemodiversity of dissolved organic matter in paddy soils. *Environ. Sci. Technol.* 52 (3), 963–971. doi: 10.1021/acs.est.7b00377

Liu, S. M., Zhang, J., Chen, H., Wu, Y., Xiong, H., and Zhang, Z. (2003). Nutrients in the changjiang and its tributaries. *Biogeochem.* 62 (1), 1–18. doi: 10.1023/A:1021162214304

Li, Y., Xu, C., Chung, K. H., and Shi, Q. (2015). Molecular characterization of dissolved organic matter and its subfractions in refinery process water by Fourier transform ion cyclotron resonance mass spectrometry. *Energy Fuels* 29 (5), 2923–2930. doi: 10.1021/acs.energyfuels.5b00333

Lu, Y. H., Bauer, J. E., Canuel, E. A., Chambers, R., Yamashita, Y., Jaffé, R., et al. (2014). Effects of land use on sources and ages of inorganic and organic carbon in temperate headwater streams. *Biogeochem.* 119 (1), 275–292. doi: 10.1007/s10533-014-9965-2

Martin, R. A., and Harrison, J. A. (2011). Effect of high flow events on in-stream dissolved organic nitrogen concentration. *Ecosystems* 14 (8), 1328–1338. doi: 10.1007/s10021-011-9483-1

McKnight, D. M., Boyer, E. W., Westerhoff, P. K., Doran, P. T., Kulbe, T., and Andersen, D. T. (2001). Spectrofluorometric characterization of dissolved organic matter for indication of precursor organic material and aromaticity. *Limnol. Oceanogr.* 46 (1), 38–48. doi: 10.4319/lo.2001.46.1.0038

Medeiros, P. M., Seidel, M., Ward, N. D., Carpenter, E. J., Gomes, H. R., Niggemann, J., et al. (2015). Fate of the Amazon river dissolved organic matter in the tropical Atlantic ocean. *Global Biogeochem. Cycles* 29 (5), 677–690. doi: 10.1002/2015GB005115

Ohno, T. (2002). Fluorescence inner-filtering correction for determining the humification index of dissolved organic matter. *Environ. Sci. Technol.* 36 (4), 742–746. doi: 10.1021/es0155276

Painter, S. C., Lapworth, D. J., Woodward, E. M. S., Kroeger, S., Evans, C. D., Mayor, D. J., et al. (2018). Terrestrial dissolved organic matter distribution in the north Sea. *Sci. Total Environ.* 630, 630–647. doi: 10.1016/j.scitotenv.2018.02.237

Pang, Y., Wang, K., Sun, Y., Zhou, Y., Yang, S., Li, Y., et al. (2021). Linking the unique molecular complexity of dissolved organic matter to flood period in the Yangtze river mainstream. *Sci. Total Environ.* 764, 142803. doi: 10.1016/j.scitotenv.2020.142803

Raeke, J., Lechtenfeld, O. J., Tittel, J., Oosterwoud, M. R., Bornmann, K., and Reemtsma, T. (2017). Linking the mobilization of dissolved organic matter in catchments and its removal in drinking water treatment to its molecular characteristics. *Water Res.* 113, 149–159. doi: 10.1016/j.watres.2017.01.066

Raeke, J., Lechtenfeld, O. J., Wagner, M., Herzsprung, P., and Reemtsma, T. (2016). Selectivity of solid phase extraction of freshwater dissolved organic matter and its effect on ultrahigh resolution mass spectra. *Environ. Sci.: Processes Impacts.* 18, 918–927. doi: 10.1039/c6em00200e

Raymond, P. A., Saiers, J. E., and Sobczak, W. V. (2016). Hydrological and biogeochemical controls on watershed dissolved organic matter transport: Pulse-shunt concept. *Ecology* 97 (1), 5–16. doi: 10.1890/14-1684.1

Richard, L. A., Lapworth, D. J., Magnone, D., Gooddy, D. C., Chambers, L., Williams, P., et al. (2019). Dissolved organic matter tracers reveal contrasting characteristics across high arsenic aquifers in Cambodia: A fluorescence spectroscopy study. *Geosci. Front.* 10 (5), 1653–1667. doi: 10.1016/j.gsf.2019.04.009

Riedel, T., Zark, M., Vähätalo, A., Niggemann, J., Spencer, R., Hernes, P., et al. (2016). Molecular signatures of biogeochemical transformations in dissolved organic matter from ten world rivers. *Front. Earth Sci.* 4. doi: 10.3389/feart.2016.00085

Rivas-Ubach, A., Liu, Y., Bianchi, T. S., Tolic, N., Jansson, C., and Pasa-Tolic, L. (2018). Moving beyond the van krevelen diagram: A new stoichiometric approach for compound classification in organisms. *Anal. Chem.* 90 (10), 6152–6160. doi: 10.1021/acs.analchem.8b00529

Roebuck, J. A., Seidel, M., Dittmar, T., and Jaffe, R. (2020). Controls of land use and the river continuum concept on dissolved organic matter composition in an anthropogenically disturbed subtropical watershed. *Environ. Sci. Technol.* 54, 195–206. doi: 10.1021/acs.est.9b04605

Roth, V. N., Dittmar, T., Gaupp, R., and Gleixner, G. (2013). Latitude and pH driven trends in the molecular composition of DOM across a north south transect along the yenisei river. *Geochim. Cosmochim. Acta* 123, 93–105. doi: 10.1016/j.gca.2013.09.002

Seidel, M., Yager, P. L., Ward, N. D., Carpenter, E. J., Gomes, H. R., Krusche, A. V., et al. (2015). Molecular-level changes of dissolved organic matter along the Amazon river-to-Ocean continuum. *Mar. Chem.* 177, 218–231. doi: 10.1016/j.marchem.2015.06.019

Shang, Y., Song, K., Jacinthe, P.-A., Wen, Z., Zhao, Y., Lyu, L., et al. (2021). Fluorescence spectroscopy of CDOM in urbanized waters across gradients of Development/Industrialization of China. *J. Hazard. Mater.* 415, 125630. doi: 10.1016/j.jhazmat.2021.125630

Singh, S., Dash, P., Silwal, S., Feng, G., Adeli, A., and Moorhead, R. J. (2017). Influence of land use and land cover on the spatial variability of dissolved organic matter in multiple aquatic environments. *Environ. Sci. pollut. Res.* 24 (16), 14124–14141. doi: 10.1007/s11356-017-8917-5

Sleighter, R. L., Cory, R. M., Kaplan, L. A., Abdulla, H. A., and Hatcher, P. G. (2014). A coupled geochemical and biogeochemical approach to characterize the bioreactivity of dissolved organic matter from a headwater atream. *J. Geophys. Res. Biogeosci.* 119 (8), 1520–1537. doi: 10.1002/2013JG002600

Stedmon, C. A., and Bro, R. (2008). Characterizing dissolved organic matter fluorescence with parallel factor analysis: A tutorial. *Limnol. Oceanogr. Methods* 6 (11), 572–579. doi: 10.4319/lom.2008.6.572

Stubbins, A., Lapierre, J. F., Berggren, M., Prairie, Y. T., and Dittmar, T. (2014). What's in an EEM? molecular signatures associated with dissolved organic fluorescence in Boreal Canada. *Environ. Sci. Technol.* 48. doi: 10.3389/feart.2015.00063

Stubbins, A., Spencer, R. G., Chen, H., Hatcher, P. G., Mopper, K., Hernes, P. J., et al. (2010). Illuminated darkness: Molecular signatures of Congo river dissolved organic matter and its photochemical alteration as revealed by ultrahigh precision mass spectrometry. *Limnol. Oceanogr.* 55 (4), 1467–1477. doi: 10.4319/lo.2010.55.4.1467

Stubbins, A., Spencer, R. M., Mann, P. J., Holmes, R. M., McClelland, J. W., Niggemann, J., et al. (2015). Utilizing colored dissolved organic matter to derive dissolved black carbon export by arctic rivers. *Front. Earth Sci* 3. doi: 10.3389/feart.2015.00063

Su, S., Xie, Q., Smith, A. J., Lang, Y., Hu, W., Cao, D., et al. (2022). A new structural classification scheme for dissolved organic sulfur in urban snow from north China. *Environ. Sci. Technol. Lett.* 9 (5), 366–374. doi: 10.1021/acs.estlett.2c00153

Vannote, R. L., Minshall, G. W., Cummins, K. W., Sedell, J. R., and Cushing, C. E. (1980). The river continuum concept. *Canadian Journal of Fisheries and Aquatic Sciences* 37, 130–137. doi: 10.1139/f80-017

Wagner, S., Riedel, T., Niggemann, J., Vähätalo, A. V., Dittmar, T., and Jaffé, R. (2015). Linking the molecular signature of heteroatomic dissolved organic matter to watershed characteristics in world rivers. *Environ. Sci. Technol.* 49 (23), 13798–13806. doi: 10.1021/acs.est.5b00525

Wang, X., Ma, H., Li, R., Song, Z., and Wu, J. (2012). Seasonal fluxes and source variation of organic carbon transported by two major Chinese rivers: The yellow river and changjiang (Yangtze) river. *Global Biogeochem. Cycles* 26 (2), 1–10. doi: 10.1029/2011GB004130

Wang, K., Pang, Y., He, C., Li, P., Xiao, S. , Sun, Y., et al. (2019b). Optical and molecular signatures of dissolved organic matter in xiangxi bay and mainstream of three gorges reservoir, China: Spatial variations and environmental implications. *Sci. Total Environ.* 657, 1274–1284. doi: 10.1016/j.scitotenv.2018.12.117

Wang, X., Wu, Y., Bao, H., Gan, S. , and Zhang, J. (2019a). Sources, transport, and transformation of dissolved organic matter in a Large river system-illustrated by the changjiang river, China. *J. Geophys. Res. Biogeosci.* 124, 3881–3901. doi: 10.1029/2018JG004986

Williams, C. J., Frost, P. C., Morales-Williams, A. M., Larson, J. H., Richardson, W. B., Chiandet, A. S., et al. (2016). Human activities cause distinct dissolved organic matter composition across freshwater ecosystems. *Glob. Change Biol.* 22 (2), 613–626. doi: 10.1111/gcb.13094

Wu, Y., Bao, H., Yu, H., Zhang, J., and Kattner, G. (2015). Temporal variability of particulate organic carbon in the lower changjiang (Yangtze river) in the post-three gorges dam period: Links to anthropogenic and climate impacts. *J. Geophys. Res. Biogeosci.* 120, 2194–2211. doi: 10.1002/2015JG002927

Wünsch, U. J., Acar, E., Koch, B. P., Murphy, K. R., Schmitt-Kopplin, P., and Stedmon, C. A. (2018). The molecular fingerprint of fluorescent natural organic matter offers insight into biogeochemical sources and diagenetic state. *Anal. Chem.* 90, 14188–14197. doi: 10.1021/acs.analchem.8b02863

Wu, Y., Zhang, J., Liu, S., Zhang, Z., Yao, Q., Hong, G., et al. (2007). Sources and distribution of carbon within the Yangtze river system. *Estuar. Coast. Shelf Sci.* 71, 13–25. doi: 10.1016/j.ecss.2006.08.016

Yamashita, Y., Kloeppel, B. D., Knoepp, J., Zausen, G. L., and Jaffé, R. (2011). Effects of watershed history on dissolved organic matter characteristics in headwater streams. *Ecosystems* 14, 1110–1122. doi: 10.1007/s10021-011-9469-z

Yu, K., Gan, Y., Zhou, A., Liu, C., Duan, Y., and Han, L. (2018). Organic carbon sources and controlling processes on aquifer arsenic cycling in the jianghan plain, central China. *Chemosphere* 208, 773–781. doi: 10.1016/j.chemosphere.2018.05.188

Yu, H., Wu, Y., Zhang, J., Deng, B., and Zhu, Z. (2011). Impact of extreme drought and the three gorges dam on transport of particulate terrestrial organic carbon in the changjiang (Yangtze) river. *J. Geophys. Res. Earth Surface* 116, 1–15. doi: 10.1029/2011JF002012

Zhang, A., Zhang, J., and Liu, S. (2020). Spatial and temporal variations of dissolved silicon isotope compositions in a Large dammed river system. *Chem. Geol.* 545, 119645. doi: 10.1016/j.chemgeo.2020.119645

Zhou, Y., Yao, X., Zhou, L., Zhao, Z., Wang, X., Jang, K., et al. (2021). How hydrology and anthropogenic activity influence the molecular composition and export of dissolved organic matter: Observations along a Large rive continuum. *Limnol. Oceanogr.* 66, 1730–1742. doi: 10.1002/lno.11716